

DETERMINATION OF THE FATIGUE STRENGTH OF A RAILWAY VEHICLE NODE USING THE PROBABILITY APPROACH

Jaroslav Václavík*, Pavel Marek**, Jan Chvojan*, Miloslav Kepka***

This paper presents a case study for the strength demonstration of a railway wagon welded node using the probability approach. The design variables were taken from the existing standardization for railway vehicles. The fatigue damage summation method for proving the satisfactory service life as well as the Goodman diagram method for verification of the unlimited service life was used for the node examination. The probability estimation was made using the Monte Carlo SBRA method with the help of the Anthill software.

Keywords: railway, wagon, probability, fatigue, service life, Goodman diagram, SBRA

1. Introduction

The vehicle components subject to dynamic stresses are damaged in most cases due to the fatigue process. The assessment of limited or unlimited fatigue life is often based on the deterministic approaches using the mean values and the safety coefficients. However, if these coefficients are not chosen properly, the interference between loaded stresses and the fatigue resistance of a joint can cause the fatigue damage or breaking of the material.

A goal of this article is to compare the semi-probabilistic approach for determination of the railway vehicle fatigue strength used in UIC specifications [1] with the fully probabilistic approach using a simulation based reliability assessment access which is demonstrated on a chosen railway vehicle welded node.

2. The approach based on the UIC standards

Before a new type of rail vehicle is put into service, the structural tests are carried out on the body and the bogie frame of the prototype or one of the first production components. These tests are described in detail in several UIC leaflets with the exception of the general testing conditions which are common to the different tests and the permissible limit values.

The procedure used is based on the structure limit states given in [1]. The object of [1] specification is especially to verify the fatigue strength with the help of the static tests using two coefficients K (0.2 or 0.3 depending on a vehicle type) of dynamic stressing. The resistance against fatigue is verified using two methods in the above mentioned document :

* Ing. J. Václavík, Ing. J. Chvojan, ŠKODA VÝZKUM s.r.o., Tylova 1/57, 316 00 Plzeň

** prof. Ing. P. Marek, DrSc., ÚTAM AVČR, Prosecká 76, 190 00 Praha

*** doc. Ing. M. Kepka, CSc., ZČU v Plzni, FS, KKS, Univerzitní 22, 306 14 Plzeň

- a. The fatigue damage summation method by means of a cumulative damage calculation according to the Miner rule for the stress spectrum resulting from the load spectrum and its comparison with the allowable value $D = 1$.
- b. A computation of the maximum amplitude and its mean value from the stress time history with the help of the dynamic stress coefficients and their comparison with the fatigue endurance limit using
 - i. the Goodman diagram,
 - ii. a S-N curves stress amplitude according to [4] for $N = 2 \times 10^6$ cycles.

The resistance against permanent deformation is verified in [1] using the allowable stress defined as a yield point of the welded joint divided by 1.1.

The S-N curves and the Goodman diagrams as well as the tabled limit stresses (a stress range, the mean stress and the maximum stress) are given in [1] for unalloyed steel for different notch cases. A different approach should be mentioned for determination of stresses using both approaches. The nominal stresses are used for calculation of the fatigue damage while near hot-spot stresses are used for the approach using the Goodman diagram. The tabled fatigue limit stresses are derived from the Goodman diagrams and from the S-N curves for $N = 2 \times 10^6$ cycles for two coefficients K of dynamic stressing. The limits for the case a. correspond to the values contained in the Eurocode [4] for a life 2×10^6 stress reversal under the single-stage load spectrum for 95 % survival probability. The limit values for the case b. were partially taken from [2] and divided by the factor 1.25 for the survival probability of 99.7 %.

3. The probability approach using SBRA

The existing standards, codes and specifications ([1], [2], [3] and [4]) are based on the partial safety factors (including especially uncertainties of the stress history and the material characteristics) using the semi-probabilistic approach and having in common a general format of the reliability check method where the designer is acting as an interpreter of numerous prescriptions. This approach can be characterised as the safe life. In case of the damage tolerance approach where the damage is permitted after the design life the fully probabilistic method is necessary.

The fully probabilistic approach, the simulation based reliability assessment (SBRA), and the limit state design philosophy are used in the Anthill software for Windows [5]. Using the Monte Carlo simulation, the probability of failure $P_f = P(RF \leq 0)$ is obtained by analyzing the random reliability function (reserve) RF expressed as a difference between the structure resistance RV (time dependent or independent) and the load effect S random variables ($RF = RV - S$). The empirical distribution of RF is generated step-by-step by using distributions of the input random variables RV , S after many simulation steps. According to [4] the design failure probability is recommended to be 7.2×10^{-5} ; in case of serviceability assessment the design failure probability is equal to 6.7×10^{-2} .

In this article the structure resistance RV is expressed as an ultimate limit state and is represented by i) a material elasticity limit, ii) a node fatigue limit (both considering as time-independent) and iii) a time dependent $RV(t)$ accumulation of damage $AD = 1 - Ad_{ac}/Ad_{tol}$. The safety of the structure is expressed by comparing the calculated probability with the design target probability of failure for the unlimited life or the design service life.

4. A measured object and obtained time histories

4.1. Test conditions

The object of investigation was a welded node used in the prototype of a freight car for the passenger vehicles transport documented at the Figure 1 (a connection of two I-beams at the end of a triangular rib). It concerns the end of the welded radius beam going from the cross beam to the longitudinal beam. The type of the notch was the class 36 (i.e. a stress range at 2×10^6 cycles) for the fatigue damage summation method (see also [4]) and the case D for the Goodman diagram method, both according to [1]. The strain gauge was placed on the longitudinal beam just for measuring the nominal stress.

The service test was performed on the railway line Kolín – Nymburk – Praha Libeň – Běchovice – Cerhenice being approximately 120 km long. The data acquisition was made with a mobile measuring unit with a sampling frequency of 800 Hz and a low-pas filter 100 Hz.

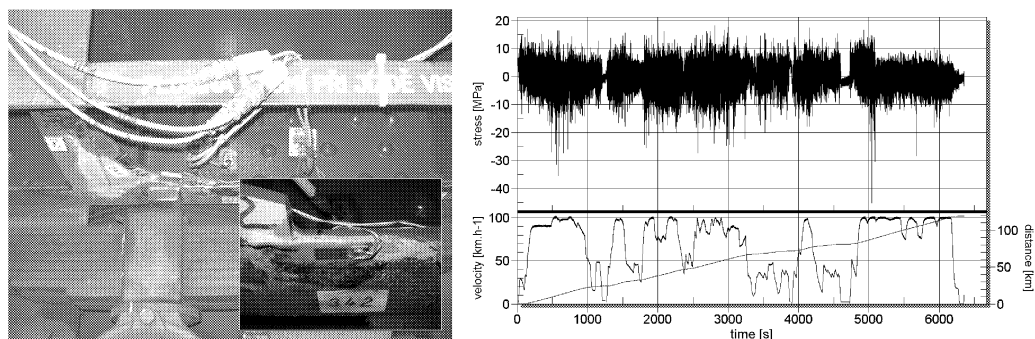


Fig.1: The measured welded node of the wagon skeleton and the time histories of node normal stress, the wagon velocity and travelled distance

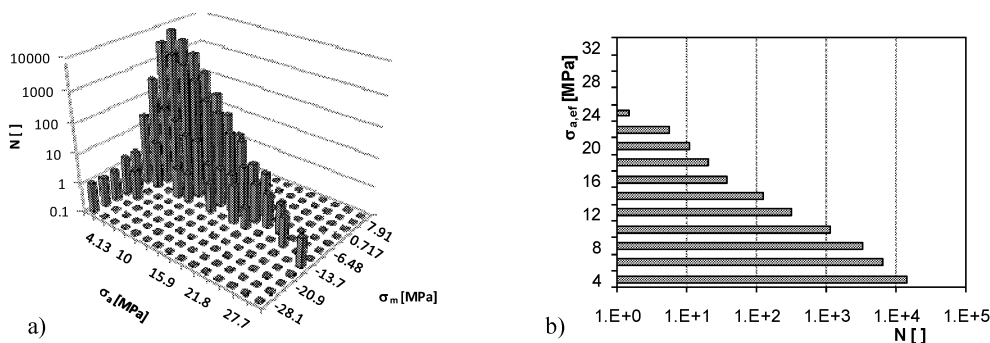


Fig.2: The measured 3-D histogram of the stress amplitudes (a) and the 2D histogram of the recalculated effective stress amplitudes (b)

4.2. Measured data processing

A two-parametric histogram of the stress amplitude rate was processed from the measured stress time history using the rain-flow method (Figure 2a). Using the sensitivity for the mean stress M (here chosen $M = 0.11$ according to the Goodman diagram [1]) where the

influence of the static mean stress σ_m is taken into account by increasing the stress amplitude $\sigma_{a,i}$ to $\sigma_{a,ef,i}$, this histogram was recalculated to the one-dimensional one according to the relation (1). The resulting histogram is given at the Figure 2b.

$$\sigma_{a,ef,i} = \sigma_{a,i} + M \sigma_m . \quad (1)$$

4.3. Extrapolation of the histogram of the stress amplitudes

The last five histogram classes contain less than 1.5 amplitude cycles; one of them is not occupied at all. It is expected that the distribution of the stress amplitudes could significantly change due to increasing the length of the test inside these classes.

For that reason the distribution of these extreme stress amplitudes was estimated according to the procedure proposed in [7]. The whole time history was divided into 24 non-overlapping segments with the length of 4.96 km and the distribution of the stress amplitude extremes $F(\sigma_a)$ taken from each segment was approximated using the Weibull type of distribution (see the Figure 3).

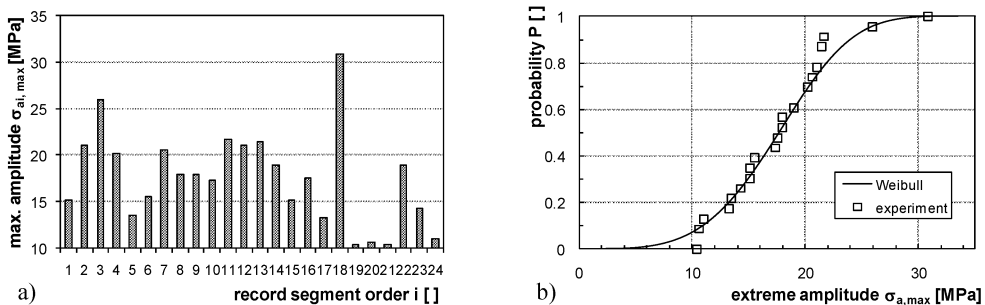


Fig.3: The extreme amplitudes in each segment (a) and the amplitude approximation using the Weibull distribution (b)

Several values of found stress amplitude distribution $[1 - F(\sigma_a)]$ for higher classes are given in the Table 1. The estimation of a cycle number in these classes was calculated using the following consideration [7]. The probability of amplitude presence in the given segment or its higher value is given with the complement of the distribution function. A reciprocal value of this probability is equal to a number d of segments which are necessary for an appearance of the amplitude once a time or for its exceeding

$$d(\sigma_{a, \max}) = \frac{100}{1 - F(\sigma_{a, \max})} \quad [\%] . \quad (2)$$

Thus, $d = 2$ segments are necessary for the extreme value which should be exceeded with the probability $P = 50\%$ and $d = 10$ segments are necessary, if the probability should be $P = 10\%$. If the length of the segment is l , the necessary length for satisfying this condition is $d \times l$. A number of repetition n of the given class stress amplitude $\sigma_{a, \max, i}$ will be

$$n(\sigma_{a, \max, i}) = \frac{l_{\text{tot}}}{d(\sigma_{a, \max, i}) l} . \quad (3)$$

class i	$\sigma_{a,i}$ [MPa]	$F(\sigma_{a,i})$ [-]	$1 - F(\sigma_{a,i})$ [-]	$n_{i, \text{approx}}$ [cycles]	$n_{i, \text{orig}}$ [cycles]
11	21.8	0.794810604	0.205189	4.924546	5.5
12	23.8	0.892994313	0.107006	2.568136	1.5
13	25.7	0.951233457	0.048767	1.170397	1
14	27.7	0.982631927	0.017368	0.416834	1
15	29.7	0.995146282	0.004854	0.116489	0
16	31.6	0.99888107	0.001119	0.026854	1
17	33.6	0.999824795	0.000175	0.004205	0
18	35.6	0.999979791	2.02E-05	0.000485	0
19	37.5	0.999998403	1.6E-06	3.83E-05	0
20	39.5	0.999999917	8.29E-08	1.99E-06	0
21	41.5	0.999999997	2.71E-09	6.51E-08	0
22	43.4	1	5.33E-11	1.28E-09	0

Tab.1: Extrapolation of the stress amplitude histogram

An approximated expected number of cycles n_i , approx calculated according to the above mentioned considerations for the length $l_{\text{tot}} = 119.089 \text{ km}$ is given in the Table 1. The comparison is performed with the originally measured cycle numbers $n_{i, \text{orig}}$.

Other considerations are made to find out how an omission of the fracture part of the cycles in higher classes can influence the estimated service life. The partial damage D_i and life L_i were computed for each amplitude class which are shown at the Figure 4a. The corresponded cumulative values of damage are shown at the Figure 4b. The computation was made from the original stress spectrum with addition of the extrapolated classes from the Table 1.

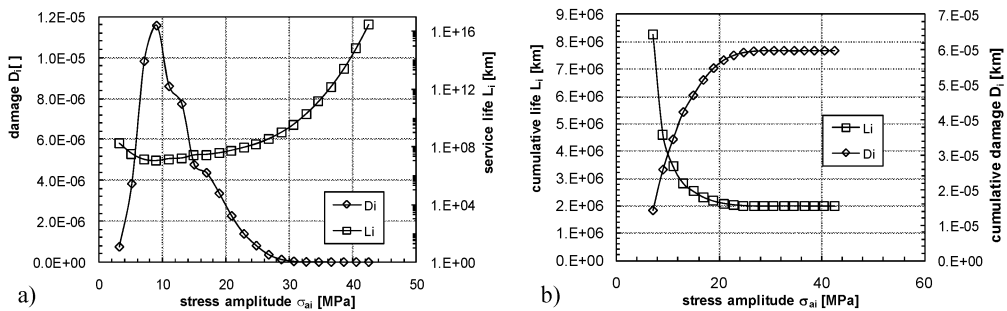


Fig.4: Contribution of the individual classes to the final life (a) and the corresponding cumulative values (b)

The highest damage is caused for the stress amplitude class $i = 5$ with the amplitude $\sigma_a = 10 \text{ MPa}$; the damage is negligible above the class $i = 13$ for the amplitudes over $\sigma_a = 25 \text{ MPa}$. An interesting conclusion is that the extrapolated spectrum does not give a considerable improvement of the estimated service life for the given service condition.

5. Representation of input variables in the probability domain

5.1. Stress time history

The histogram of the stress history was used to check the stress towards plastic deformations, for other cases the histogram of the stress amplitudes was used.

When using the Goodman diagram, the measured stress history was multiplied by two to estimate an increase of the measured nominal stress values at the weld toe.

The extrapolated histogram of stress amplitudes was used for the probabilistic calculations based on the fatigue limit or the damage accumulation. However, it should be mentioned that the obtained results with the extrapolated or original histogram are nearly the same. Besides the above mentioned considerations, a reason of this is caused by the fact that it is not possible to enter the numbers of the histogram with an exponent lower than 10^{-5} . For that reason it is not possible to enter the histogram rates whose mean value is close to 1. The distribution function of the stress amplitudes from the stress history is given at the Figure 5.

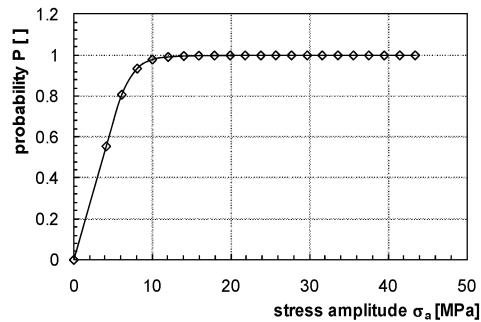


Fig.5: Distribution of the effective stress amplitudes

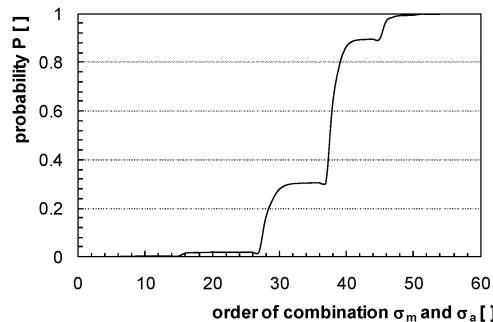


Fig.6: Distribution of the combination σ_m and σ_a

An estimation of distribution of cycles n_i inside each stress amplitude class $\sigma_{a,i}$ was performed using the distribution function. The method used here is based on the step-by-step random generation of new rain-flow matrices from the original two-parametric matrix [10] using the inverse of the distribution function given at the Figure 6. Then, the distribution of the stress amplitudes was calculated from the set of the rain-flow matrices, obtained this way, for several amplitude levels. These distributions were entered to the Anthill program in the form of the stress amplitude histogram rates in the individual files. The histograms are visualized at the Figure 7. For the classes higher than 16 the histograms were too thin; they were replaced with theoretical distributions where the variability of n_i was entered with the class mean value and the standard deviation was estimated with the help of the trend of the variation coefficient.

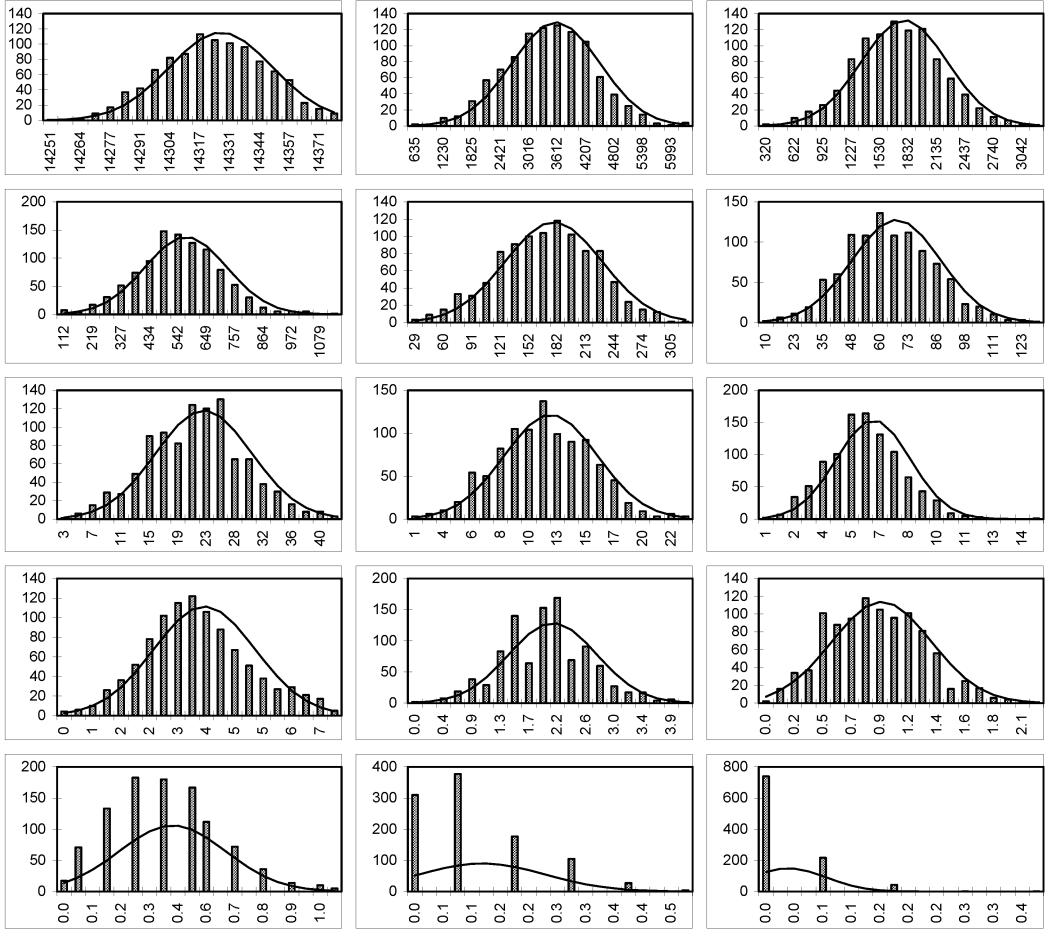


Fig.7: Histograms of the stress amplitude $\sigma_{a,i}$ rates and their approximation to the normal distributions

5.2. Material characteristics

5.2.1. Yield point

A yield point of the used material is taken from [2] $R_{p0.2} = 240$ MPa for 50% probability. We assume the normal distribution of this limit. Its variation was estimated according to the results given in [8] $V_{R_{p0.2}} = 0.053$ which gives the standard deviation $s(R_{p0.2}) = 12.72$ MPa.

5.2.2. Fatigue limit

We assume the log-normal distribution of the stress cycles N a standard deviation of which is estimated from [9] for the filled weld type W to be $s(\log N) = 0.184$. The standard deviation of the fatigue limit can be calculated according to the relation

$$s(\log \sigma_c) = \frac{s(\log N_c)}{m}, \tag{4}$$

where m is a slope of the S-N curve.

- a) The stress amplitude at the fatigue limit taken from the S-N curve is $\sigma_{c,95} = 16$ MPa for 95 % probability (the nominal approach). Going out from the given standard deviation and 95 % fractile, the mean value can be calculated using the inverse log-normal distribution, $\sigma_{c,50} = 25.7$ MPa.
- b) The stress amplitude at the fatigue limit taken from the Goodman diagram for the stress ratio $R = -1$ and $\sigma_m = 0$ is $\sigma_c = 33$ MPa for 99.7 % probability (nearly the hot-spot value) which corresponds to $\sigma_c = 59.7$ MPa for 50 % probability. For $\sigma_m \neq 0$ the effective stress amplitude was calculated with the relation (1) instead of using the whole diagram. In (1), the following relation is valid between M and the slope φ of the upper line of the Goodman diagram

$$M = \frac{1 - \varphi}{\varphi} . \quad (5)$$

5.2.3. S-N curve

The S-N curve taken from [1] is in conformity with the codes [3] and [4]. The curve is bi-linear without a constant part, unlimited from the bottom. The values given here correspond to the left-sided tolerance limits which determine the amount of 95 % of the basic population with 75 % probability. A model with the log-normal distribution of a number of cycles N to failure was used. The variability of N is determined using the standard deviation $s(\log N)$ for the fractile d according to the given probability of failure. The following relation is given for the S-N curve

$$\log N_i = \log C_1 - m \log \sigma_{s,i} + d s(\log N) , \quad (6)$$

where C_1 is a shift of the S-N curve along the horizontal N axis, according to the used detail class given in [9], m is a slope of the S-N curve, $s(\log N)$ is a residual standard deviation of $\log N$, d is a fractile for the left-sided tolerance limit and the given probability.

The median value for the fatigue limit was calculated from the median value of a knee point $N_{c,50}$:

$$\log N_{c,50} = \log N_{c,95} + 1.645 s(\log N) , \quad (7)$$

$$\sigma_{c,50} = \sigma_{c,94} \left(\frac{N_{c,50}}{5E6} \right)^{\frac{1}{m}} . \quad (8)$$

The following parameters characterize the S-N curve:

Knee point :	$N_{c,95} = 5E6$ MPa,
Stress amplitude for 95 % survival probability :	$\sigma_{c,95} = 13$ MPa,
Stress amplitude for 50 % survival probability :	$\sigma_{c,50} = 16.41$ MPa,
Slope of S-N curve :	for $N < N_c$ $m = 3$, for $N > N_c$ $m = 5$,
Standard deviation of $\log N$:	$s(\log N) = 0.184$.

6. Calculation of welded node strength using the probability approach

6.1. Resistance against permanent deformation

The reliability function is expressed as a difference between the yield point and the node operational stress history each given as a multiple of the median value and the random

variable. The random variables are entered using the distribution parameters ($R_{p0.2}$) and the histogram of stresses (σ).

$$RF = RV - Q = (R_{p0.2 \text{ nom}} \times R_{p0.2 \text{ var}}) - (\sigma \text{ nom} \times \sigma \text{ var}) . \quad (9)$$

The form of the probability density functions of both variables and its mutual position on the stress axis is shown at the Figure 8a. The reliability function calculated with the Anthill program in the histogram form is given at the Figure 8b.

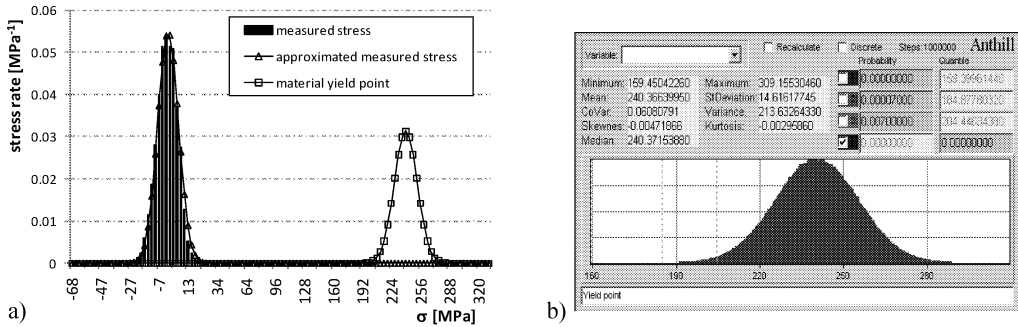


Fig.8: Resistance against the yield point stress

6.2. Resistance against the unlimited service life

The reliability function is expressed as a difference between the fatigue limit stress amplitude (the normal distribution) (used from the S-N curve or the Goodman diagram) and the node operational stress amplitude history (entered as a histogram). The used Goodman diagram and extreme values at the individual stress amplitude classes are given at the Figure 9a. The charts of probability density functions of both distributions are given at the Figure 10.

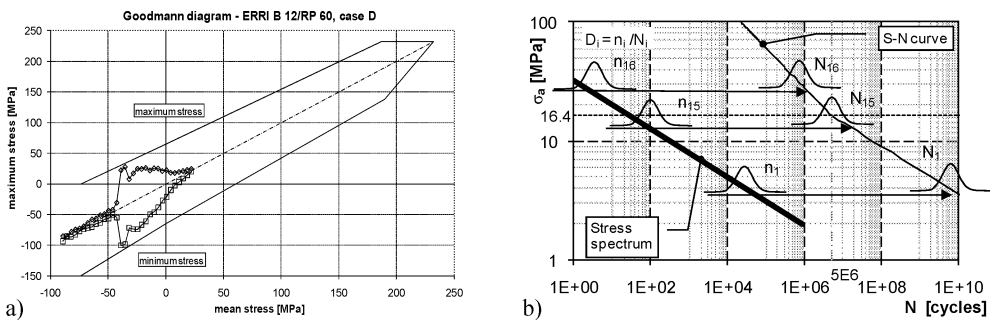


Fig.9: The Goodman diagram with the measured extreme stresses inside the individual classes (a) and the method for accumulation damage calculation inside the Anthill program (b)

The Anthill resulting histogram of the reliability function is given at the Figure 11. The resulting probability of failure is $P = 0.001$ for the fatigue limit taken from the S-N curve and $P = 3 \times 10^{-5}$ for the fatigue limit taken from the Goodman diagram. The probabilities are lower than it corresponds to the fatigue curves given in the standard.

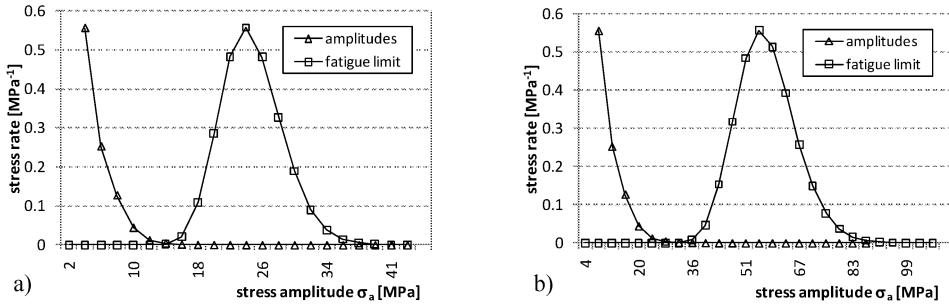


Fig.10: The probability densities of the stress history and the fatigue limit, (a) according to the Eurocode and (b) according to the Goodman diagram [1]

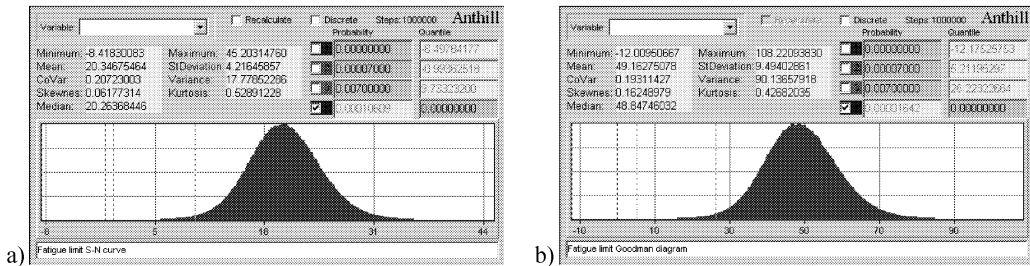


Fig.11: The reliability function for the fatigue strength against the fatigue limit according to the Eurocode (a) and the Goodman diagram (b)

6.3. Service Life Estimation Using the Accumulated Damage

The use of the Anthill program for the damage accumulation is more complicated than the procedure used in the previous chapters. The reliability function describes the state of damage history. The damage unit corresponds to the measured loop of the length $l = 119.093$ km. This distance caused the damage D_b . The distance L_1 comprised of the b_1 units, $L_1 = b_1 l$ causes the damage $S = b_1 D_b = L/(l D_b)$. The limit value $D_M = 1$ corresponds to the reference value RV . The reliability function is expressed as a residual life according to the following relation

$$RF = D_M - \frac{L_1}{l} D_b = 1 - \frac{L_1}{l} D_b . \tag{10}$$

The variable L – the estimated service life – is calculated according to the relation

$$L = \frac{l}{\sum_{i=1}^{21} D_i} = \frac{l}{D_b} . \tag{11}$$

The stress amplitude classes are entered as independent variables $S1$ to $S21$ with the uniform distribution. The numbers to failure are entered as the variables $N1$ to $N21$ either using the histogram files or with the parameters of the normal distribution. The variability of the S-N curve is given with the help of the variability of a knee point N_c through $s(\log N)$. The variables $a1$ to $a21$ are proportional to the damage at the individual stress amplitude class levels; the variable a is proportional to the total damage. These individual variables are used because it is not possible to use cycles inside the Anthill program. The calculation process is visualised at the Figure 9b. The graphical output given from the Anthill program

is shown at the Figure 12. A resulting distribution function of the service life is given at the Figure 13.

The failure of the node is expected after 565×10^3 km with the probability of 99.7%.

7. Conclusions

The node under investigation does not fulfil the unlimited service life as it was found out using the probability approach and the damage accumulation method. The failure is expected after 565×10^3 km with the probability of 99.7% and 940×10^3 km with the probability of 95%.

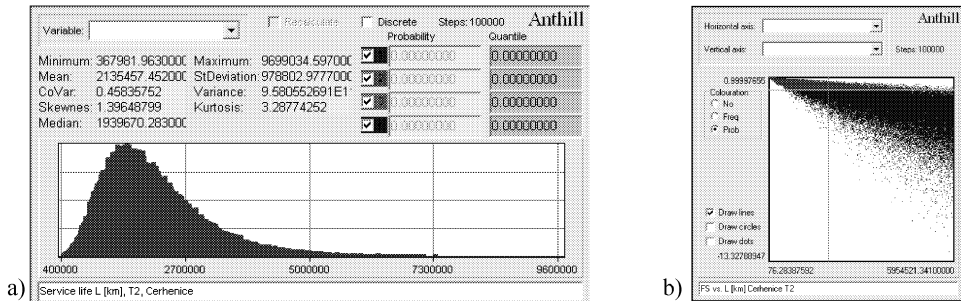


Fig.12: The outputs from the Anthill program, (a) the histogram of service life L and (b) the reliability function RF – the accumulation damage in dependence on the travelled distance

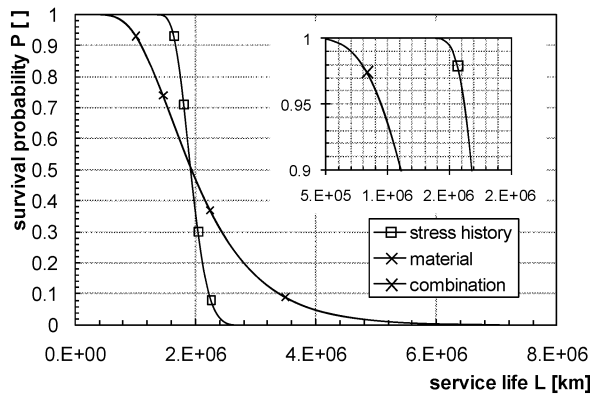


Fig.13: The resulting distribution function of the service life with the detail in the area of low damage

The performed estimation is expressively influenced by the variation of the S-N curve parameters (which were estimated) while the influence of variability of the driving conditions is nearly insignificant (the stress was measured for a representative long track). If the variability of the S-N curve is omitted, the service life is increased up to 1.4 mil.km. The standard deviation of the service life estimation is 978 000 km, if only the variation of the S-N curve is accepted, while the one makes 215 000 km, if only the variability of the service condition is considered. The median value of the service life is equal to 1.9 mil. km for both

cases. For more reliable and accurate estimation the S-N curve should be given on the basis of the test.

This conclusion is in contradiction with the results obtained from the approach in which the fatigue resistance is verified by means of the stress amplitude spectrum comparison with the constant fatigue limit. For both approaches, as for using the fatigue limit from the S-N curve and as for the Goodman diagram the probability of failure is very low and the condition for unlimited life is fulfilled with a high probability ($P > 1 \times 10^{-3}$). On the basis of the performed study the investigated node was recommended for redesigning.

Acknowledgements

The support of the MSM 1M0519 Research centre of rail vehicles and grant GACR 103/07/0557 of Czech Science Foundation is highly appreciated.

References

- [1] Tests to demonstrate the strength of railway vehicles, Regulations for proof test and maximum permissible stresses, ERRI B 12/RP 60 Utrecht, June 1995
- [2] Programme of tests to be carried out on wagons with steel under frame and body structure (suitable for being fitted with the automatic buffing and draw coupler) and on their cast steel frame bodies, ERRI B 12/RP 17, 8th Edition, Utrecht, April 1997
- [3] Hobbacher A.: Fatigue design of welded joints and components, Recommendations of IIW Joint Working Group XIII-XV, XIII-1539-96/XV-845-96, Abington Publishing, 1996
- [4] ČSN EN 1993-1-9 73 1401 Eurokód 3: Navrhování ocelových konstrukcí – Část 1-9: Únava, ČNI, 2006
- [5] Marek P., Guštar M., Anagnos T.: Simulation-Based Reliability for Structural Engineers, CRC Press, Inc., Boca Raton, Florida, 1995
- [6] Marek P., Vlk M.: Probabilistic assessment of the fatigue life of tubular steel supports of Žďákov bridge, Sborník konference Engineering mechanics, 2006
- [7] Buxbaum O.: Betriebsfestigkeit, sichere und wirtschaftliche Bemessung schwingbruchgefaehrdeeter Bauteile, Verlag Stahleisen mbH, Duesseldorf, 1988
- [8] Kmet S.: Hodnoty návrhovej pravdepodobnosti Pfd, Sb. VI. Konf. Spolehlivost konstrukcí, Dům techniky Ostrava, 6 April, 2005, in Czech
- [9] Code of practice for Fatigue design and assessment of steel structures, British standard BS 7608:1993
- [10] Culek B., Jr., Culek B.: Probabilistic assessment of the service life of undercarriage railway frame, Procc. of the int. conf. Reliability and diagnostics of transport structures and means, University of Pardubice, 26–27 September, 2002

Received in editor's office: March 2, 2010

Approved for publishing: June 14, 2010